Linear Thermoelastic Characterization of Anisotropic Poly(ethylene terephthalate) Films

Ru Feng, Richard. J. Farris

Polymer Science and Engineering Department, University of Massachusetts Amherst, Amherst, Massachusetts 01003

Received 24 September 2001; accepted 13 February 2002

ABSTRACT: All nine independent elastic constants have been determined for a biaxially stretched poly(ethylene terephthalate) (PET) film using novel mechanical methods. The orthotropic directions and the in-plane Poisson's ratios were first characterized using vibrational holographic interferometry of tensioned membrane samples. The out-of-plane Poisson's ratio was obtained by measuring the change in tension with the change in pressure for constant strain conditions. Pressure–volume–temperature (PVT) equipment was used to measure the bulk compressibility as well as the volumetric thermal expansion coefficient (TEC). The in-plane Young's moduli were obtained by tensile tests, while the out-of-plane modulus was calculated from the compressibility and other elastic constants that describe the in-plane behavior. The in-plane TECs in the machine and transverse directions were determined using a thermal mechanical analyzer (TMA). The out-of-plane TEC was determined using these values and the volumetric TEC determined via PVT. The resulting compliance matrix satisfies all of the requirements of a positive-definite energy criterion. The procedure of characterization utilized in this article can be applied to any orthotropic film. © 2002 Wiley Periodicals, Inc. J Appl Polym Sci 86: 2937–2947, 2002

Key words: polyester; films; mechanical properties; thermal properties

INTRODUCTION

Biaxially oriented poly(ethylene terephthalate) (PET) film is a semicrystalline material with good strength, toughness, flexibility, chemical resistance, electrical insulation, and dimensional stability. It is widely used in applications such as magnetic recording, photographic films, drafting films, flexible electrical circuits, and packaging materials. The tenter frame-processed PET film is anisotropic in nature, which means it has different material properties in different in-plane and out-of-plane directions. Moreover, due to the low crystallinity and the existence of molecular orientation in the noncrystalline regions, the film is in a so-called metastable state.[1] Residual stress and latent free energy formed during processing can cause large stresses or shrinkage of the materials in later usage, especially upon heating. A complete characterization of the mechanical and thermal properties of the material is needed to perform the stress analysis of coating systems, which can predict the stress state and reliability of the material in complex applications.

In the small-strain and linear elastic region, a generalized Hooke's law shown in eq. (1) can be applied to describe the material's response. For an orthotropic material,[2] 12 constants are required to describe the thermal and mechanical properties once the orthotropic axes are determined. These represent nine independent compliances and three thermal expansion coefficients (TECs). As shown in Figure 1, direction **3** is perpendicular to the plane of the film. Direction **1** and direction **2** are close to the machine direction (MD) and the transverse direction (TD).

$$\begin{bmatrix} \varepsilon_{11} - \alpha_1\Delta T \\ \varepsilon_{22} - \alpha_2\Delta T \\ \varepsilon_{33} - \alpha_3\Delta T \\ 2\varepsilon_{12} \\ 2\varepsilon_{13} \\ 2\varepsilon_{23} \end{bmatrix} = \begin{bmatrix} C_{11} & C_{12} & C_{13} & 0 & 0 & 0 \\ C_{12} & C_{22} & C_{23} & 0 & 0 & 0 \\ C_{13} & C_{23} & C_{33} & 0 & 0 & 0 \\ 0 & 0 & 0 & C_{44} & 0 & 0 \\ 0 & 0 & 0 & 0 & C_{55} & 0 \\ 0 & 0 & 0 & 0 & 0 & C_{66} \end{bmatrix} \begin{bmatrix} \sigma_{11} \\ \sigma_{22} \\ \sigma_{33} \\ \sigma_{12} \\ \sigma_{13} \\ \sigma_{23} \end{bmatrix} \quad (1)$$

$$C_{11} = 1/E_{11} \quad C_{44} = 1/G_{12} \quad C_{12} = C_{21} = -\nu_{12}/E_{11} = -\nu_{21}/E_{22}$$
$$C_{22} = 1/E_{22} \quad C_{55} = 1/G_{13} \quad C_{13} = C_{31} = -\nu_{13}/E_{11} = -\nu_{31}/E_{33}$$
$$C_{33} = 1/E_{33} \quad C_{66} = 1/G_{23} \quad C_{23} = C_{32} = -\nu_{23}/E_{22} = -\nu_{32}/E_{33}$$

ε_{ij} : strain — E_{ij} : tensile modulus
σ_{ij} : stress — G_{ij} : shear moddulus
α_i : TEC — ν_{ij} : Poisson's ratio
C_{ij} : compliance

Scheme 1: Generalized Hooke's law for orthotropic materials.

Compared with the in-plane properties, the out-of-plane elastic constants are much more difficult to determine. Special techniques are usually required for these measurements. Tong et al. once reported a ca-

Correspondence to: R. J. Farris.

Contract grant sponsors: MRSEC Central Research Facilities; UMass CUMIRP Program.

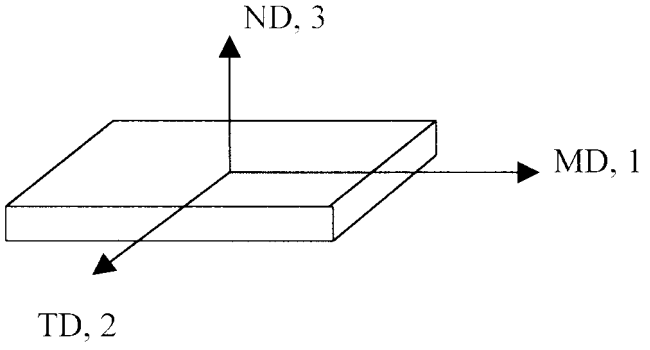

Figure 1 Cartesian axes with respect to the film plane.

pacitance-change technique (CC technique) to measure the TEC in the thickness direction.[3] In the CC technique, the polymer film was sandwiched between two flat fused quartz plates, each containing a square electrode. The change of capacitance of the capacitor composed by the two electrodes can reflect the thickness change of the polymer film during thermal cycling. Tong et al. also illustrated a Fabry-erot laser interferometric technique. In this technique, a reflective substrate and a beamsplitter layer were used instead of electrode plates as in the CC technique. Film thickness change was determined by measuring the interfering reflected intensity, which was caused by the changing phase difference between the interfering reflections between the sandwich layers. Further, Tong et al. used a thermal-mechanical analyzer (TMA) with a push-rod dilatometer attached to multilayered films.

However, it should be noted that the change in the thickness of the coatings attached to a substrate with either temperature or normal stress does not directly measure the out-of-plane TEC or the modulus in the thickness direction. The proper definition of such constants can only be derived from the equation of state, which requires thermal expansion to be measured at constant stress and moduli to be measured under specific stress states. Both of these conditions are violated when working with coatings. Raumann determined the five elastic constants of a transversely isotropic PET film by a "25-s (square) stress cycle" measurement. Three of the constants were calculated from the Young's moduli, E_0, E_{45}, and E_{90}, and the other two from the torsional moduli, G_0 and G_{90}.[4] Ward et al. obtained the thickness compliance of films by measuring the compressional strain change of narrow strips, cut in specific directions as a function of the applied hydrostatic pressure in a compressional creep apparatus.[5] All Poisson's ratios are obtained by direct measurement of the dimension change with the help of specially designed optical techniques.[6] Ward et al. also used torsional and simple-shear methods to measure the shear compliances of PET sheets.[7] In this article, the out-of-plane properties are calculated from the bulk properties, and the in-plane properties, using relations between the elasticity coefficients derived from the equation of state.[8]

THEORY

Vibrational holographic interferometry

Developed in our research lab, vibrational holographic interferometry is not only an excellent method of studying residual stress as a function of temperature or humidity in polymer coatings, but also a powerful technique for thin-film characterization, such as the determination of the principal orthotropic directions and the measurements of the in-plane Poisson's ratios. The technique has been fully described elsewhere.[8,9] It is based on the fact that a polymer membrane, in a state of tension, will resonate at characteristic frequencies when excited by a piezoelectric shaker. With a special holographic camera, unique displacement patterns can be observed at the resonant frequencies, which are related to the stress stored in the polymeric film by eq. (2):

$$\sigma_{11}^{2D}m^2 + \sigma_{22}^{2D}n^2 = 4\rho L^2 f_{mn}^2 + D\left(\frac{\pi}{L}\right)^2 (n^2 + m^2)^2 \quad (2)$$

where σ_{11}^{2D} and σ_{22}^{2D} are biaxial stresses in the two principal directions (MPa); ρ, the material density (kg/m^3); L, the square membrane length (m); f_{mn}, the resonant frequency for the (m,n) mode (Hz); and D, the flexural rigidity; $D = \{(Eh^2)/[12(1 - \nu^2)]\}$ for an isotropic material for biaxially tensioned square membranes; and by eq. (3):

$$\sigma^{1D} = 4\rho L^2\left(\frac{f_i}{i}\right)^2 - D\left(\frac{\pi}{L}\right)^2 i^2 \quad (3)$$

where σ^{1D} is the uniaxial stress (MPa); L, the length of the ribbon sample (m); and f_i, the resonant frequency for i^{th} mode (Hz) for uniaxially tensioned ribbon samples. To our knowledge, this is the only direct method that can be utilized to measure the residual stress of anisotropic materials. Furthermore, the symmetric properties of the patterns also determine the principal directions, or orthotropic axes, of the material, which normally do not correspond to the machine and transverse directions for commercial films that are produced via a tenter frame. The latter point is very important as an orthotropic material using the orthotropic axes as a reference only requires 12 coefficients. An orthotropic material not using the orthotropic axis for reference requires 27 constants to fully describe the thermoelastic behavior.

For large, thin, and highly tensioned membranes, the factor D, which describes rigidity effects, is not important. Due to the stiffness and thickness of the

material tested in our study, this bending effect of the film cannot be ignored. For aniostropic materials, square membranes are used to measure the 2D stress in the two principal directions, σ_{11} and σ_{22}. The 1D stress can then be determined by ribbon samples cut along the two specific directions. Finally, the in-plane Poisson's ratio can be calculated using the following relations:

$$\nu_{12} = \frac{(\sigma_{11}^{2D} - \sigma_{11}^{1D})}{\sigma_{22}^{2D}}$$
$$\nu_{21} = \frac{(\sigma_{22}^{2D} - \sigma_{22}^{1D})}{\sigma_{11}^{2D}} \quad (4)$$

Another advantage of this technique is that no other physical properties of the material are required to determine the Poisson's ratio.

High-pressure gas dilatometry

The dilatometry developed by Farris in the 1960s was used to measure the out-of-plane Poisson's ratios, ν_{13} and ν_{23}, of the PET film. By applying a hydrostatic pressure (P) to a narrow ribbon sample which is held at constant strain with one end attached to a load cell, the change in stress (σ) with the hydrostatic pressure can be measured. For a sample cut in direction **1**,

$$\varepsilon_{11} = C_{11}\sigma_{11} + C_{12}\sigma_{22} + C_{13}\sigma_{33} \quad (5)$$

As the sample was only uniaxially stretched, $\sigma_{11} = \sigma - P$ and $\sigma_{22} = \sigma_{33} = -P$, eq. (5) can be modified to obtain

$$\frac{\varepsilon_{11}}{C_{11}} = \sigma - P\left(1 + \frac{C_{12}}{C_{11}} + \frac{C_{13}}{C_{11}}\right) \quad (6)$$

Differentiating the equation with respect to pressure yields

$$\left(\frac{\partial\sigma}{\partial P}\right) = 1 - \nu_{12} - \nu_{13} \quad (7)$$

Since the in-plane Poisson's ratio, ν_{12}, can be obtained by holographic interferometry, the out-of-plane Poisson's ratio can be calculated from eq. (7), once the slope of the stress versus the hydrostatic pressure is measured. Similarly, by cutting the sample in direction **2**, ν_{23} can also be calculated from eq. (8):

$$\left(\frac{\partial\sigma}{\partial P}\right)_{\varepsilon_{22}} = 1 - \nu_{21} - \nu_{23} \quad (8)$$

Pressure–volume–temperature (PVT)

The volumetric TEC, α_v, and the bulk compressibility, κ, can be determined by a Gnomix Inc. PVT apparatus.[10] The volume change of a sample, as a function of temperature and hydrostatic pressure, can be measured by this instrument. According to linear elastic theory,

$$\varepsilon_{11} - \alpha_1\Delta T = C_{11}\sigma_{11} + C_{12}\sigma_{22} + C_{13}\sigma_{33}$$
$$\varepsilon_{22} - \alpha_2\Delta T = C_{21}\sigma_{11} + C_{22}\sigma_{22} + C_{23}\sigma_{33}$$
$$\varepsilon_{33} - \alpha_3\Delta T = C_{31}\sigma_{11} + C_{32}\sigma_{22} + C_{33}\sigma_{33} \quad (9)$$

For a film under hydrostatic pressure, $\sigma_{11} = \sigma_{22} = \sigma_{33} = -P$, the dilatation of the volume is, by definition, the sum of the strains in all three directions, which can be presented as a function of temperature and pressure:

$$\frac{\Delta V}{V} = (\alpha_1 + \alpha_2 + \alpha_3)\Delta T - P\sum_{i,j=1}^{3} C_{ij} \quad (10)$$

In an isothermal PVT run, one can measure the volume change as a function of pressure at a series of constant temperatures:

$$-\frac{1}{V_0}\left(\frac{\partial V}{\partial P}\right)_T = \sum_{i,j=1}^{3} C_{ij} = \kappa \quad (11)$$

where κ is the bulk compressibility and

$$\sum_{i,j=1}^{3} C_{ij} = C_{11} + C_{22} + C_{33} + 2(C_{12} + C_{13} + C_{23}) \quad (12)$$

Therefore, the out-of-plane modulus can be obtained by the following calculation:

$$\frac{1}{E_{33}} = \kappa - \left[\frac{1}{E_{11}} + \frac{1}{E_{22}} - 2\left(\frac{\nu_{12}}{E_{11}} + \frac{\nu_{13}}{E_{11}} + \frac{\nu_{23}}{E_{22}}\right)\right] \quad (13)$$

In an isobaric PVT run, the pressure is kept constant, while the volume change as a function of temperature is obtained:

$$\frac{1}{V_0}\left(\frac{\partial V}{\partial T}\right)_P = \alpha_1 + \alpha_2 + \alpha_3 = \alpha_V \quad (14)$$

Since the in-plane TECs, α_1 and α_2, can be measured by TMA, the out-of-plane TEC, α_3, can be calculated from eq. (14).

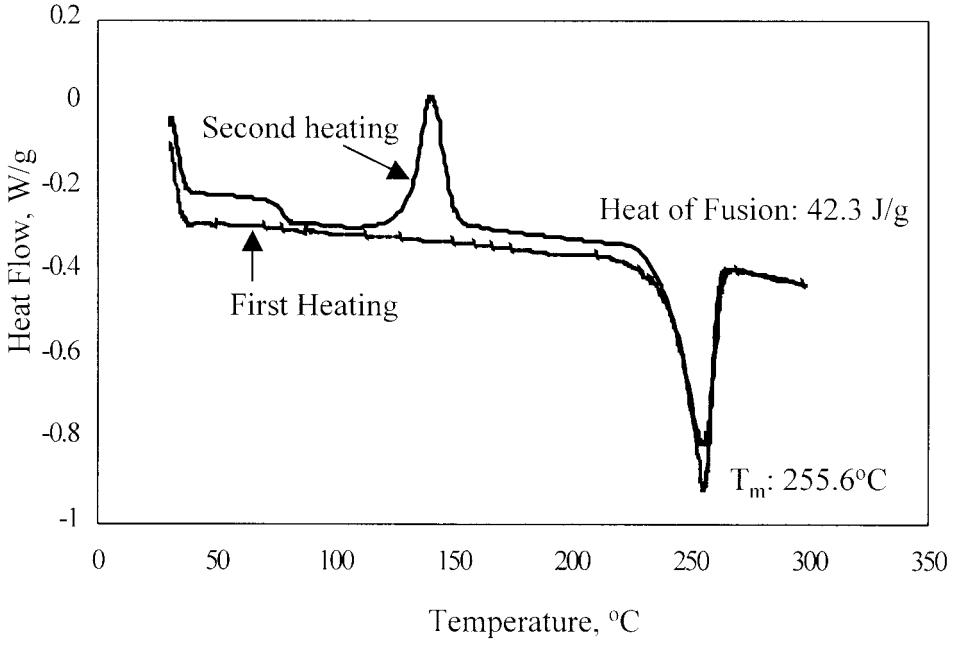

Figure 2 DSC curves of the PET film.

Torsion pendulum

In the free torsion pendulum technique, the period of oscillation of the disc mass hung on the narrow ribbon can be related to the torsional rigidity and then related to the out-of-plane shear moduli by eq. (15). For samples cut along direction **2**,

$$p^{-2} = \frac{8a^3bG_{23}}{\pi^6 IL} \sum_{m=1}^{\infty} \frac{1}{m^4} \left(1 - \frac{1}{Q_m} \tanh Q_m\right) \quad (15)$$

$$Q_m = \frac{\pi bm}{2a} \sqrt{\frac{G_{12}}{G_{23}}} \quad (16)$$

where p is the period of oscillation (s); a, the width of sample (m); b, the thickness of sample (m); L, the length of sample (m); and I, the momentum of inertia of disc (kg m^2). Similarly, G_{13} can also be determined by measuring samples cut along direction **1**. This technique is excellent for fibers, but the accuracy for relatively thick films is not the best. Determining these shear moduli is very difficult by any method and this is the best direct method that we know of at this time.

EXPERIMENTAL

Materials

The PET film provided by the Eastman Kodak Co. has a thickness of 100 μm. The density of the material was determined to be 1.393 cm^3/g by a gradient density column measurement. The crystallinity is 35.04% according to eq. (17):

$$c\% = \frac{\rho_c(\rho_s - \rho_a)}{\rho_s(\rho_c - \rho_a)} \times 100\% \quad (17)$$

where ρ_c is the density of pure crystal of PET, ρ_c = 1.515 cm^3/g (ref. 11); ρ_a, the density of pure amorphous PET, ρ_a = 1.335 cm^3/g (ref. 11); and ρ_s, the density of the PET sample.

From the DSC curve in Figure 2, the melting point of the material was determined to be 255.6°C. The crystallinity calculated from the DSC measurement is 33.50% since

$$c\% = \frac{\Delta H_f^s}{\Delta H_f^0} \times 100\% \quad (18)$$

∇H_f^0 is the heat of fusion for the pure crystal of PET, ∇H_f^0 = 126.4 J/g (ref. 12), and ∇H_f^s is the heat of fusion of the PET sample, ∇H_f^s = 42.3 J/g.

Real-time vibrational holographic interfermetry

For anisotropic films, a circular membrane was first made and tested using vibrational holographic interferometry. The principal directions were determined from the symmetry of the holographic patterns for circular samples. These directions can deviate from the MD and TD by as much as 20°. A square membrane with its sides parallel to the principal directions was then made and tested to get the 2D stress of the membrane. A 1D constrained thin ribbon was made by cutting the square membrane in either direction **1** or **2**. The 1D stress was then measured by holographic

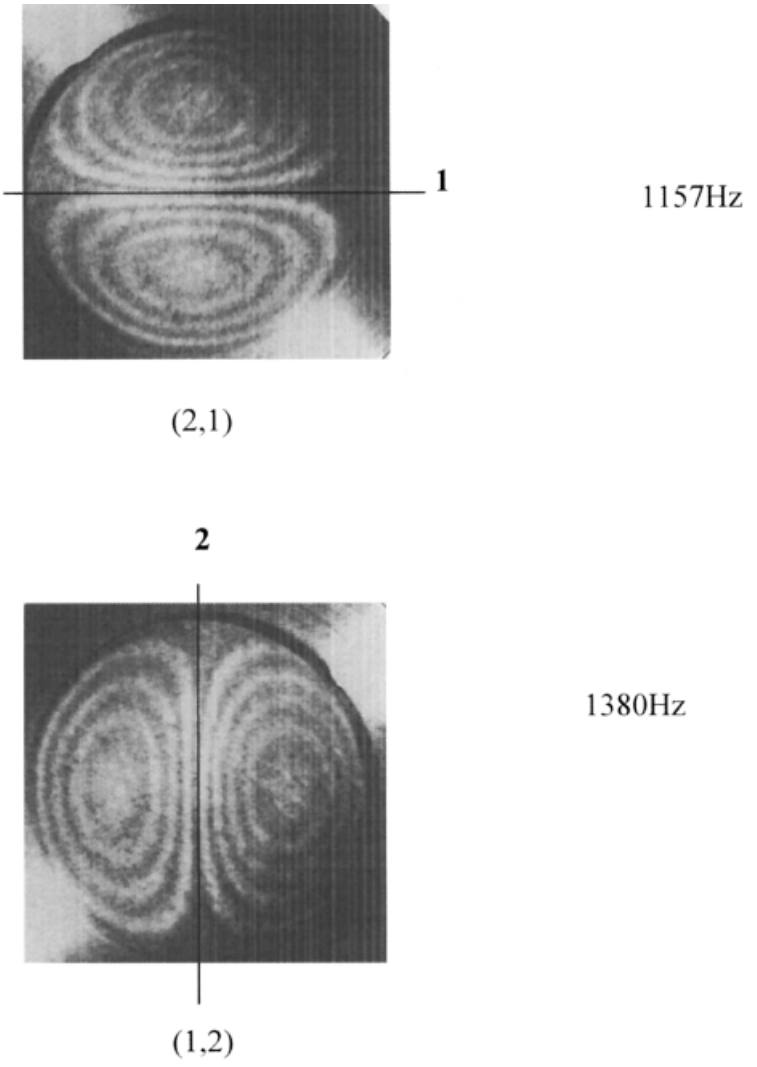

Figure 3 Determination of the orthotropic directions.

interferometry. The experiments were carried out at room temperature under high vacuum conditions.

PVT tests

About 1 g of PET film was stacked and rolled and then placed into the rigid sample cell of the PVT apparatus. The void space of the sample cell was then filled with mercury. The temperature of the sample was measured by a thermocouple and the pressure was controlled by an Enerpac P-2282 hand pump. The change in sample volume was detected by the movement of a bellows at the bottom of the sample cell, which was connected to a linear variable differential transducer (LVDT). The cross-sectional area of the bellows was 1.145 cm^2. The isothermal run was done at a temperature range of 30–75°C, with the pressure being changed from 10 to 60 MPa at intervals of 5 MPa. The PVT apparatus had a high sensitivity of 0.0005 cm^3/g and a good accuracy of ± 0.002 cm^3/g at the test temperature range.

Tensile tests

Using ASTM D882-88 guidelines,[13] all tensile tests were done on an Instron tensile tester, Model 4468, with a 1 KN load cell. Samples were cut along the measured principal directions as well as several other directions into 5 × 0.5-cm ribbons. The crosshead speed used was 5 mm/min. Eight to ten specimens were tested for each direction and the average value was reported.

Thermal analysis

The in-plane TECs, α_1 and α_2, were determined using a TA Instruments TMA 2940. Samples with a dimen-

TABLE I
Measurement of the In-plane Poisson's Ratios

m	n	f_{mn} (kHz)	σ^{2D} (MPa)	i	f_i (kHz)	σ^{1D} (MPa)	Poisson's ratio
1	1	2.144					
2	1	3.565		2	2.418		
2	2	4.438	$\sigma_{11}^{2D} = 8.91$	3	3.829		
1	3	5.049	$\sigma_{22}^{2D} = 7.93$	4	5.056	$\sigma_{11}^{1D} = 4.49$	$\nu_{12} = 0.39 \pm 0.02$
4	2	7.583	$D = 6.61$	5	7.684	$D = 8.24$	
3	3	6.830					
1	1	2.739					
1	2	4.351		4	6.342		
1	3	6.252	$\sigma_{11}^{2D} = 12.89$	5	8.062		
2	1	4.470	$\sigma_{22}^{2D} = 13.98$	6	10.492	$\sigma_{22}^{1D} = 7.75$	$\nu_{21} = 0.48 \pm 0.02$
3	1	6.386	$D = 5.07$	7	12.808	$D = 7.62$	
3	2	7.309		9	17.754		
1	4	8.236					
2	4	9.152					
4	4	11.951					
6	2	13.625					

The values of m, n, and f are only one set of the measurements, while D, σ, and ν are the average values of several different measurements.

sion of 5 × 25 mm were used in the measurements. A small force (0.1 or 0.02 N) was applied to the sample to prevent it from wrinkling during the dimension measurements. Nitrogen with a flow rate of 60 mL/min was used to purge the sample while heating. The sample was heated to 75°C at a heating rate of 5°C/min several times to erase the heating history of the sample . The linear TEC was calculated over the temperature range of 30–70°C.

High-pressure gas dilatometry

A ribbon sample of 5 mm in width and 6–7 cm in length cut in either direction **1** or direction **2** was

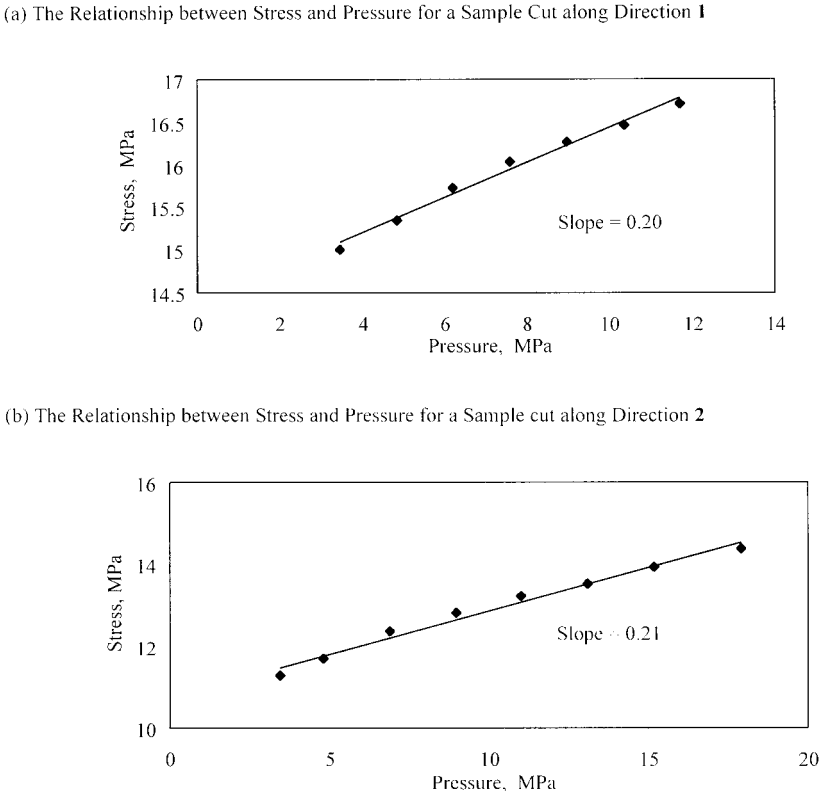

Figure 4 Measurement of the out-of-plane Poisson's ratios.

TABLE II
Measurement of the Out-of-plane Poisson's Ratios

Direction	Slope ($\partial\sigma/\partial P$)	Poisson's ratio
1	0.20 ± 0.02	$\nu_{13} = 0.41 \pm 0.02$
2	0.21 ± 0.02	$\nu_{23} = 0.31 \pm 0.02$

placed in a high-pressure chamber. The sample was held at a constant strain (~0.5%) with one end attached to a load cell, which was utilized to determine the stress in the sample. Stress changes, as a function of hydrostatic pressure from atmospheric pressure to 18 MPa, were measured.

Torsion pendulum

Very narrow ribbon (~0.3 mm in width and ~5 cm in length) samples were tested on a torsion pendulum apparatus. The sample was fixed at one end, with the other end attached to a circular disk having a moment of inertia of 106 g mm^2. The disk was rotated manually and then released, and the period of the free oscillation was recorded.

RESULTS AND DISCUSSION

Principal direction and in-plane poisson's ratio

Figure 3 shows the (1, 2) and (2, 1) modes of holographic patterns. The principal directions can be determined from the symmetry of these patterns. It was found that the angle between the principal directions and the reference directions (MD or TD) changed from one sheet of film to another, indicating a product that is not homogeneous. Normally, these directions are known to vary across the width of a tenter frame line.[14] In the middle of the frame, the orthotropic directions are usually identical to the MD and TD, but the angle between MD and direction **1** (or TD and direction **2**) can be as great as 20° near the edges.

A square membrane, with its sides parallel to the principal directions, was then made and the 2D stresses of the membrane were measured. A constrained 1D thin ribbon was made by cutting the membrane in either direction **1** or direction **2**, and the 1D stress was then measured by holographic interferometry. Several replicate tests were performed for each measurement, and the average of the results was used. The calculated results are shown in Table I. The measured D value is close to an estimated value according to the equation $D = \{(Eh^2)/[12(1 - \nu^2)]\}$, which is around 6.5.

Out-of-plane poisson's ratios

The change of stress as a function of hydrostatic pressure from atmospheric pressure to 18 MPa (using nitrogen gas) was recorded and is shown in Figure 4. The stress increased linearly with the hydrostatic pressure. The out-of-plane Poisson's ratios were calculated from eqs. (6) and (7) and the results are shown in Table II.

In-plane moduli

The elastic moduli, E_{11} and E_{22}, can be determined by tensile tests of the samples, where cuts were made in directions **1** and **2**, respectively. Table III shows the tensile test results for samples cut in direction **1**, direction **2**, and a direction that has a 45° angle to direction **1**. Samples cut in other directions were also tested. The Young's moduli in different in-plane directions, E_θ, are shown in Figure 5. The largest error for tensile tests came from the area measurement of the samples, since E_θ is related to θ by

$$\frac{1}{E_\theta} = \frac{\cos^4\theta}{E_{11}} + \frac{\sin^4\theta}{E_{22}} + \frac{1}{4}\left[\frac{1}{G_{12}} - \frac{2\nu_{12}}{E_{11}}\right]\sin^2 2\theta \quad (19)$$

The calculated values of the moduli, according to eq. (19), in different directions are also shown in Figure 5. It was found that, besides observing two relative maximum at $\theta = 0°$ and $\theta = 90°$ in the range of [0°, 90°], there is a relative minimum at $\theta \sim 40°$.

Assume that

$$A = \frac{1}{E_{11}}, \qquad B = \frac{1}{E_{22}}, \qquad C = \frac{1}{4}\left(\frac{1}{G_{12}} - \frac{2\nu_{12}}{E_{11}}\right),$$

Equation (19) can be simplified to

TABLE III
Tensile Tests Results

Measurement	Direction		
	1	**2**	45° to **1**
Stress at break (MPa)	156.9	185.9	176.2
Strain at break (%)	92.28	90.74	96.74
Modulus (GPa)	$E_{11} = 3.9 \pm 0.2$	$E_{22} = 4.7 \pm 0.2$	4.0 ± 0.2

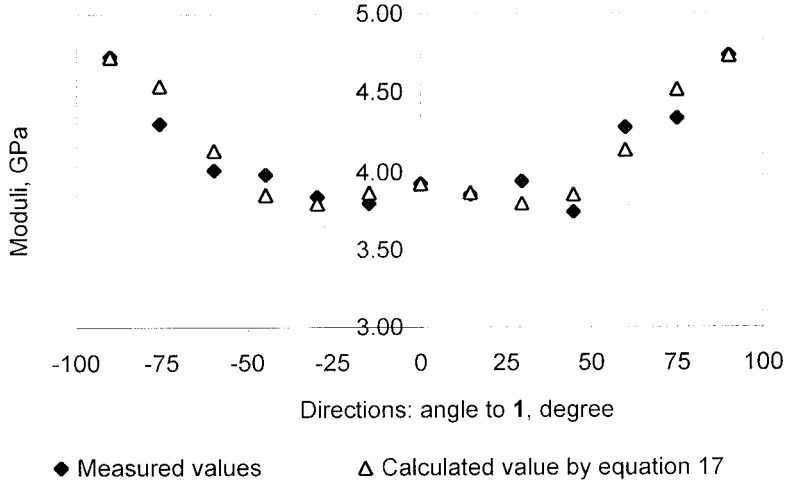

Figure 5 Moduli for different in-plane directions of the film.

$$f(\theta) = \frac{1}{E_\theta} = A\cos^4\theta + B\sin^4\theta + C\sin^2 2\theta \quad (20)$$

At the angle at which E_θ reaches its relative maximum or minimum value, the first derivative of $f(\theta)$ should be zero. So,

$$f'(\theta) = -4A\cos^3\theta\sin\theta + 4B\sin^3\theta\cos\theta + 4C\sin 2\theta\cos 2\theta = 4\cos\theta\sin\theta(-A\cos^2\theta + B\sin^2\theta + 2C\cos 2\theta) = 0 \quad (21)$$

This can be satisfied under either of the following three conditions:

1. $\theta = 0^o$, $\sin\theta = 0$.
2. $\theta = 90^o$, $\cos\theta = 0$.
3. $-A\cos^2\theta + B\sin^2\theta + 2C\cos 2\theta = 0$

$$\Rightarrow tg^2\theta = \frac{2C - A}{2C - B}$$
$$\theta = \text{arctg}\left(\pm\sqrt{\frac{2C - A}{2C - B}}\right) \quad (22)$$

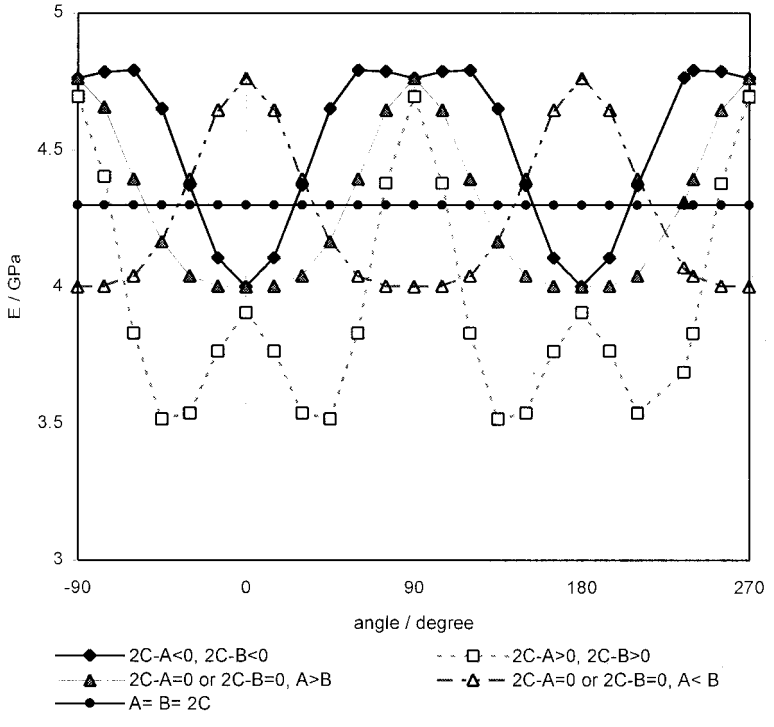

Figure 6 Five possibilities of function $E(\theta) \sim \theta$

TABLE IV
Calculation of the In-plane Modulus G_{12}

E_θ	θ	G_{12} (GPa)
3.8	15	1.21
4.1	30	1.51
4.0	45	1.37
4.4	60	1.45
4.2	75	1.21
3.8	−15	1.21
3.8	−30	1.31
4.0	−45	1.37
4.0	−60	1.24
4.1	−75	0.89[a]
		$G_{12} = 1.3 \pm 0.4$ GPa

[a] Excluded data during calculation for G_{12}.

Therefore, there are three possible relative extrema for E_θ when θ changes in the range of [0°, 90°]. However, when $2C - A = 0$ or $2C - B = 0$, θ becomes 0° or 90°, respectively, and there will be only two relative extrema in those cases. Whether the extrema is a relative maximum or a relative minimum will be decided by the value of the second derivative of the function at that point:

$$f''(\theta) = 4\cos 2\theta(-A\cos^2\theta + B\sin^2\theta + 2C\cos 2\theta) + 4\cos\vartheta\sin\theta[2A\cos\theta\sin\theta + 2B\sin\theta\cos\theta - 4C\sin 2\theta] \quad (23)$$

when $\theta = 0°$,

$$f''(\theta) = = 4(2C - A) \quad (24)$$

and when $\theta = 90°$,

$$f''(\theta) = = 4(2C - B) \quad (25)$$

According to eq. (22), $2C - A$ and $2C - B$ should either both be positive or both be negative, so $f(\theta)$ should have relative maximum or relative minimum values at both $\theta = 0°$ and $\theta = 90°$ when there are three relative extrema in the range [0°, 90°]. In the case of $2C - A = 0$ or $2C - B = 0$, there will be only two extrema in the discussed range. If $A > B$, $f(\theta)$ will have a relative maximum at $\theta = 90°$ and a relative minimum at $\theta = 0°$. If $A < B$, $f(\theta)$ will reach its maximum at $\theta = 0°$ and minimum at $\theta = 90°$. When $2C - A = 0$ and $2C - B = 0$ are satisfied at the same time, the material should be isotropic.

TABLE V
Measurement of the Out-of-plane Shear Moduli

Direction	Width (mm)	Length (mm)	Period (s)	G (GPa)
1	0.25	70.9	2.64	$G_{13} = 0.16 \pm 0.05$
2	0.23	68.2	2.76	$G_{23} = 0.17 \pm 0.05$

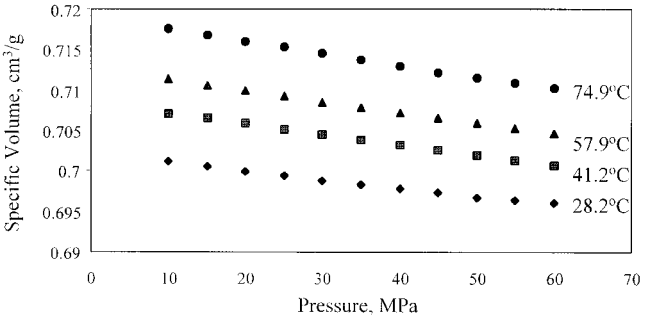

Figure 7 Measurement of the bulk compressibility.

Figure 6 shows all the five possible shapes of $E(\theta) \sim \theta$ plots. Since constants A, B, and C are, in fact, related to the modulus and Poisson's ratio directly, the actual shape of $E(\theta)$ is decided by the mechanical properties of the material. The mechanical properties of the materials are related to the orientation of the molecules, which is eventually determined by the processing conditions of the films. For films produced by a sequentially stretching processing, molecules are first oriented along the first stretching direction and then reoriented to the second stretching direction. Most likely, the $E(\theta)$ of the resultant films will present two relative maximums in the two stretching directions and a relative minimum at some angle between these two directions. The specific value of the angle will be decided by the stretching ratio in the two directions. For the film studied in this article, $A = 0.256$, $B = 0.213$, and $C = 0.167$, there are three relative extrema in the range [0°, 90°]. These include two relative maximum at $\theta = 0°$ and $\theta = 90°$ and one relative minimum at $\theta = 38.7°$. The measured $E(\theta) \sim \theta$ plot (shown in Fig. 5) has exactly the same shape as predicted, and the shape of $E(\theta) \sim \theta$ plot agrees well with the sequentially stretching processing conditions employed to produce this film. Finally, the in-plane shear modulus, G_{12}, was calculated from the tensile test results, and the results are shown in Table IV.

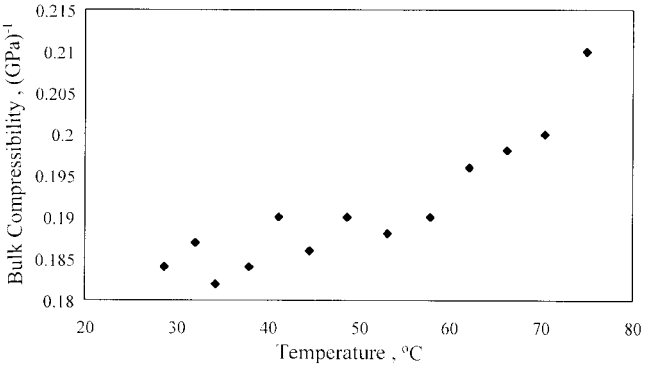

Figure 8 Bulk compressibility at different temperatures.

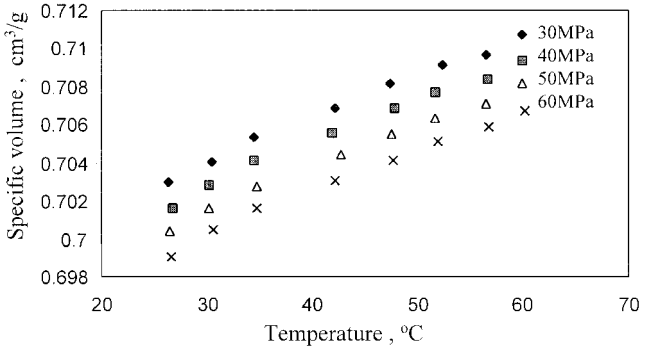

Figure 9 Specific volume change with temperature at different pressures.

Out-of-plane shear moduli

Table V shows the torsion pendulum test results. As mentioned before, the torsion pendulum does not accurately determine the shear moduli of thick films, so the data are only representative. The largest error came from the dimension measurement of the narrow ribbon samples.

Out-of-plane young's modulus and volumetric TEC

The bulk compressibility can be determined by observing the specific volume change as a function of pressure in isothermal PVT tests. Figure 7 shows the specific volume of the sample as a function of pressure at different temperatures, and the slopes of the plots yield the bulk compressibility of the material at that temperature. As shown in Figure 8, the bulk compressibility was not sensitive to the temperature when the experimental temperature was below T_g, but increased with the temperature when near or above T_g. Therefore, the bulk compressibility at room temperature was estimated as

$$\kappa = 0.184 \pm 0.003 \text{ (GPa)}^{-1}$$

Cross-plotting the data obtained from the isothermal run can give the volumetric TEC. The volume change with temperature at different pressures is plotted in Figure 9, and the slope of the plots provided the volumetric TEC. Finally, the α_v at 1 atmosphere can be obtained by extraplotting the α_v as a function of pressure as shown in Figure 10:

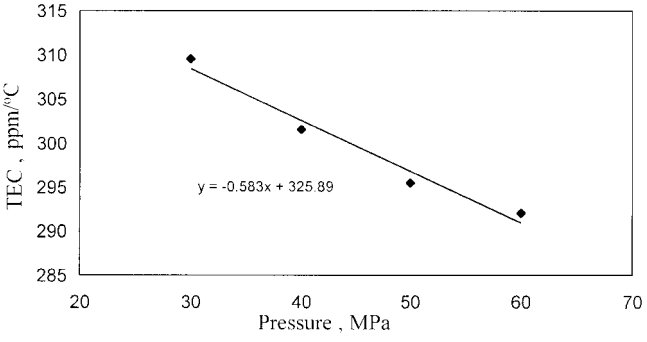

Figure 10 Calculation of the volumetric TEC at one atmosphere.

TABLE VI
TEC in Different In-plane Directions

Force = 0.1 N		Force = 0.02 N	
Angle to **1**	TEC ppm (°C)	Angle to **1**	TEC ppm (°C)
0	24.73	0	24.57
12.5	24.33	15	23.82
25	21.64	30	22.94
37.5	21.00	45	20.13
50	20.34	60	17.64
62.5	18.58	75	17.12
75	18.14	90	16.65
90	17.69	−15	24.18
−13.8	25.22	−30	22.40
−27.4	22.46	−45	20.86
−41.2	19.71	−60	19.19
−55	18.65	−75	26.98
−69	18.55		
−81	18.07		

$$\alpha_v = 326 \pm 31 \text{ ppm (°C)}$$

Finally, the out-of-plane Young's modulus can be calculated by eq. (12):

$$E_{33} = 3.9 \pm 0.7 \text{ GPa}$$

Obviously, due to the error accumulation in the calculation, the accuracy of E_{33} is not as good as that of the in-plane moduli.

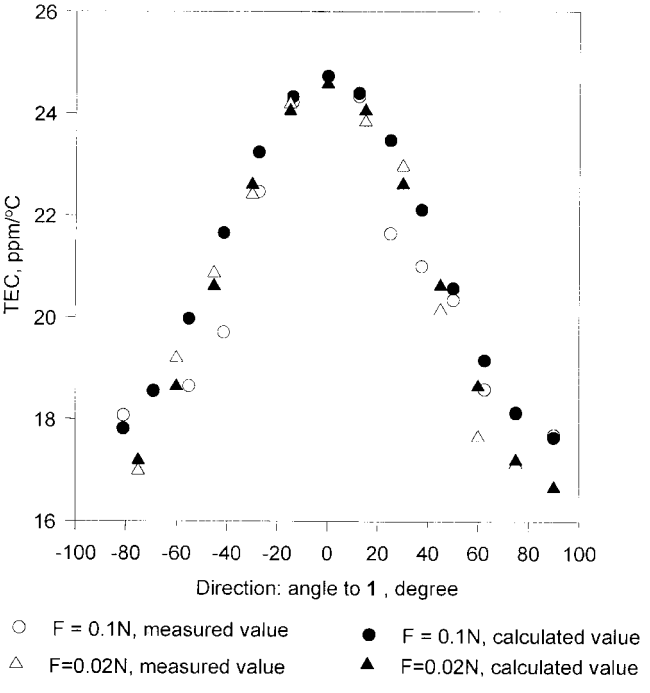

Figure 11 TEC in different in-plane directions.

TECs

Table VI summarizes two sets of TECs in different in-plane directions. It was found that the TEC increased slightly when the force applied to the sample during measurements was changed from 0.02 to 0.1 N. The difference between the measured values from direct TMA measurements and the calculated value from eq. (26) is shown in Figure 11. In comparing these values, the deviation between the calculated and the measured values increased when the applied force changed from 0.1 to 0.02 N. Sample creep might be a possible reason:

$$\alpha_\theta = \alpha_1 \cos^2\theta + \alpha_2 \sin^2\theta \qquad (26)$$

The TEC in the two in-plane principal directions were

$$\alpha_1 = 26 \pm 2 \text{ ppm } (^\circ\text{C})$$

$$\alpha_2 = 18 \pm 2 \text{ ppm } (^\circ\text{C})$$

The out-of-plane TEC was determined to be

$$\alpha_3 = \alpha_V - \alpha_1 - \alpha_2 = 282 \pm 31 \text{ ppm } (^\circ\text{C})$$

CONCLUSIONS

The compliance matrix obtained for the Kodak PET film samples is given below:

$$[C_{ij}] = \begin{bmatrix} 0.256 \pm 0.012 & -0.100 \pm 0.005 & -0.105 \pm 0.005 & 0 & 0 & 0 \\ -0.102 \pm 0.005 & 0.213 \pm 0.008 & -0.065 \pm 0.005 & 0 & 0 & 0 \\ -0.105 \pm 0.005 & -0.065 \pm 0.005 & 0.257 \pm 0.038 & 0 & 0 & 0 \\ 0 & 0 & 0 & 0.77 \pm 0.18 & 0 & 0 \\ 0 & 0 & 0 & 0 & 6.3 \pm 1.9 & 0 \\ 0 & 0 & 0 & 0 & 0 & 5.9 \pm 1.9 \end{bmatrix}$$

It should be noted that the theoretical requirements of positive-definite energy criteria for a matrix of orthotropic elastic constants include the following, all of which are satisfied:

1. $C_{11}, C_{22}, C_{33} > 0$.
2. $C_{11}C_{22} - C_{12}^2 = 0.045 > 0$.
3. $C_{11}C_{33} - C_{13}^2 = 0.055 > 0$.
4. $C_{22}C_{33} - C_{23}^2 = 0.051 > 0$.
5. $Det[C_{ij}] = 5.9 \times 6.3 \times 0.77 \times \begin{bmatrix} 0.254 & -0.100 & -0.105 \\ -0.102 & 0.213 & -0.065 \\ -0.105 & -0.065 & 0.257 \end{bmatrix} = 0.25 > 0$

Every technique used in this characterization has its own minor irreproducibility, and the estimated error for each compliance is calculated and listed in the matrix. Because the out-of-plane constants were determined in an indirect way, these values have a higher degree of uncertainty when compared to the in-plane properties. This is because of the accumulation of error in adding several values, each with its own uncertainty. For example, the thickness compliance is expressed as the difference between the bulk compressibility and five other compliances. Obviously, the maximum possible error in the thickness compliance is the sum of the maximum errors in the other compliances. These are, however, direct measurements of elasticity coefficients and are not significantly different from other methods, which require interrelations between values. We are only clearly specifying the difficulties with this and other related methods. We feel the values are quite good and very valuable for performing stress analysis calculations.

The authors would like to thank the Eastman Kodak Co., specifically Dr. Yehuda Greener and Dr. John Pochan, for their support. The authors would also like to acknowledge the support of the MRSEC Central Research Facilities and the UMass CUMIRP Program.

References

1. Blumentritt, B. F. J Appl Polym Sci 1979, 23, 3205.
2. Lai, W. M.; Rubin, D.; Krempl, E. Introduction to Continuum Mechanics; Butterworth–Heinemann: New York, 1996.
3. Tong, H. M.; Hsuen, H. K. D.; Saenger, K. L.; Su, G. W. Rev Sci Instrum 1991, 62, 422.
4. Raumann, G. Brit J Appl Phys 1963, 14, 795.
5. Wilson, I.; Cunningham, A.; Duckett, R. A.; Ward, I. M. J Mater Sci 1976, 11, 2189; Kinfayini, O. O.; Nix, E. L.; Ward, I. M. Phys E Sci Instrum 1986, 19, 911; Richardson, I.; Ward, I. M. J Polym Sci Polym Phys Ed 1978, 16, 667.
6. Ward, I. M. Plast Rubb Mater Appl 1977, Nov., 141; Wilson, I.; Ladizesky, N. H.; Ward, I. M. J Mater Sci 1976, 11, 2177; Wilson, I.; Cunningham, A.; Duckett, R. A.; Ward, I. M. J Mater Sci 1976, 11, 2189.
7. Lewis, E. L. V.; Ward, I. M. J Mater Sci 1980, 15, 2354.
8. Chen, M. J. Ph.D. Thesis, University of Massachusetts at Amherst, 1998; Tong, Q. K. Ph.D. Thesis, University of Massachusetts at Amherst, 1993; Cho, S.; Kim, G.; McCarthy, T. J.; Farris, R. J. Polym Eng Sci 2001, 4, 301.
9. Maden, M. A.; Jagota, A.; Mazur, S.; Farris, R. J. J Am Ceram Soc 1994, 77, 625.
10. Zoller, P. PVT Manual (versional 2.01); Gnomix Inc.: Boulder, CO, 1987.
11. Fakirov, S.; Fisher, E.; Schmidt, G. Makromol Chem 1975, 176, 2459.
12. Smith, C.; Dole, M. J Polym Sci 1956, 20, 37.
13. ASTM D882–88; Annual Book of ASTM, 1988.
14. Ward, I. M. Structure and Properties of Oriented Polymers, 2nd ed.; Chapman & Hall: London, 1997; p 441.